Genes & Diseases (2022) 9, 1062–1073

Available online at www.sciencedirect.com

ScienceDirect

journal homepage: http://ees.elsevier.com/gendis/default.asp

FULL LENGTH ARTICLE

BET bromodomain inhibitor JQ1 regulates spermatid development by changing chromatin conformation in mouse spermatogenesis

Xiaorong Wang [a,1], Mengmeng Sang [a,1], Shengnan Gong [a,1], Zhichuan Chen [a], Xi Zhao [a], Guishuan Wang [a], Zhiran Li [a], Yingying Huang [a], Shitao Chen [b], Gangcai Xie [a], Enkui Duan [c,**], Fei Sun [a,*]

[a] *Institute of Reproductive Medicine, School of Medicine, Nantong University, Nantong, Jiangsu 226001, PR China*
[b] *International Peace Maternity and Child Health Hospital, Shanghai Key Laboratory for Reproductive Medicine, School of Medicine, Shanghai Jiaotong University, Shanghai 200030, PR China*
[c] *State Key Laboratory of Stem Cell and Reproductive Biology, Institute of Zoology, Chinese Academy of Sciences, Beijing 100101, PR China*

Received 23 September 2020; received in revised form 18 November 2020; accepted 22 December 2020
Available online 9 January 2021

KEYWORDS
Chromatin conformation;
JQ1;
scRNA-seq;
Spermatid development;
Spermatogenesis

Abstract As a BET bromodomain inhibitor, JQ1 has been proven have efficacy against a number of different cancers. In terms of male reproduction, JQ1 may be used as a new type of contraceptive, since JQ1 treatment in male mice could lead to germ cell defects and a decrease of sperm motility, moreover, this effect is reversible. However, the mechanism of JQ1 acting on gene regulation in spermatogenesis remains unclear. Here, we performed single-cell RNA sequencing (scRNA-seq) on mouse testes treated with JQ1 or vehicle control to determine the transcriptional regulatory function of JQ1 in spermatogenesis at the single cell resolution. We confirmed that JQ1 treatment could increase the numbers of somatic cells and spermatocytes and decrease the numbers of spermatid cells. Gene Ontology (GO) analysis demonstrated that differentially expressed genes which were down-regulated after JQ1 injection were mainly enriched in "DNA conformation change" biological process in early developmental germ cells and "spermatid development" biological process in spermatid cells. ATAC-seq data

* Corresponding author.
** Corresponding author.
E-mail addresses: duane@ioz.ac.cn (E. Duan), sunfei@ntu.edu.cn (F. Sun).
Peer review under responsibility of Chongqing Medical University.
[1] These authors contributed equally to this work.

https://doi.org/10.1016/j.gendis.2020.12.012

further confirmed that JQ1 injection could change the open state of chromatin. In addition, JQ1 could change the numbers of accessible meiotic DNA double-stranded break sites and the types of transcription factor motif that functioned in pachytene spermatocytes and round spermatids. The multi-omics analysis revealed that JQ1 had the ability to regulate gene transcription by changing chromatin conformation in mouse spermatogenesis, which would potentiate the availability of JQ1 in male contraceptive.

Introduction

Mammalian spermatogenesis is a complex, elaborate and orderly process, which mainly involves three stages: the proliferation and differentiation of spermatogonia via mitosis, the production of haploid spermatids from primary spermatocytes via meiosis and spermiogenesis.[1,2] The successful completion of spermatogenesis requires the coordinated interaction of multiple genes, and their expression is precisely controlled in time and space.[3]

In mammals, the bromodomain and extra-terminal domain (BET) family is composed of BRD2, BRD3, BRD4 and BRDT. These four proteins are all involved in spermatogenesis, and BRDT is exclusively expressed in the testis.[4] BRDT initiates a programming guided by histone acetylation in meiotic and post-meiotic cells and directs the replacement of histones by transition proteins in post-meiotic cells.[5,6] BRD4 binds to the acetylated tails of histones H3 and H4[7–9] and occupies thousands of enhancers related to active genes and a small set of exceptionally large super-enhancers related to genes that feature prominently.[10–12] Studies have confirmed that super-enhancers are involved in the control of mammalian cell identity in health and in disease.[13–16]

Inhibition of BRD4 by BET bromodomain inhibitors, such as JQ1, could affect the expression of super-enhancer associated genes.[17] Furthermore, JQ1 binds competitively to the ϵ-N-acetylation of lysine residues binding site of BET family bromodomains and dramatically increases the thermal stability of all bromodomains of the BET family, but does not affect the stability of other bromodomains outside the BET family.[18] *In vivo* studies have demonstrated that intraperitoneal (*ip*) injection of JQ1 in male mice could result in impaired spermatogenesis and reduced motility. In particular, this is reversible, which means that JQ1 may be used as a potential contraceptive.[19] However, the specific mechanism of JQ1 acting on spermatogenesis and the side effects after drug treatment are still unclear.

Here, by combining single-cell RNA-seq and ATAC-seq, we demonstrated that JQ1 injection would increase the numbers of somatic cells and spermatocytes and decrease the numbers of spermatid cells. Moreover, JQ1 could modulate the expressions genes related to spermatid development by changing the chromatin conformation of germ cells in the early developmental stage to achieve the purpose of regulating spermiogenesis and sperm maturation.

Materials and methods

Experimental animals

C57BL/6 mice were purchased from Vital River Laboratories (Beijing, China) and housed in the Animal Center of Nantong University under a 12-h light/dark cycle at a temperature of 23 ± 2 °C and humidity of 50%—70%. All animal experiments were approved and conducted in compliance with the Nantong University Animal Care and Use Committee.

JQ1 and control treatment

The dosages and injection method of JQ1 and the control were based on Matzuk's description.[19] Specifically, (+)-JQ1 (ApexBio, Houston, USA; A1910) was dissolved in DMSO at 50 mg/ml and then diluted 1:10 in 10% 2-hydroxypropyl-b-cyclodextrin (Sigma, California, USA; 332607-25G), which was referred to as JQ1 in this study. JQ1 was *ip* injected into male mice at 1% of the body weight (50 mg/kg). The control was DMSO dissolved 1:10 in 10% 2-hydroxypropyl-b-cyclodextrin and *ip* injected into male mice at 1% of the body weight. Juvenile (3 weeks old) C57BL/6 male mice in these studies were weighed daily before injections.

Hematoxylin and eosin staining

Testicular tissues of WT, control and JQ1-treated mice were dissected out and fixed with 4% paraformaldehyde overnight, then embedded in paraffin wax and sectioned at 4 mm. For histological evaluation, sections were stained with hematoxylin and eosin (Sangon Biotech, Shanghai, China; E607318-0200) using standard techniques for histological evaluation.

Tissue dissociation and single-cell suspension preparation

The preparation method of single cell suspension of testis is as described in Luo's description.[20] Specifically, testes of WT, control and JQ1-treated group were removed and minced by scissors, then incubated in 10 ml DMEM (Life Technologies, NY, USA; 11995-081) containing 1 mg/ml collagenase IV (Sigma, California, USA; C5138-1G) and 1 unit/ml DNase I (Sigma, California, USA; AMPD1-1KT) in a

shaking water bath at 32 °C for 10 min. The seminiferous tubules were collected by centrifugation at 500*g* for 2 min. The pellet was washed once with DMEM and re-suspended in 10 ml DMEM containing 1 mg/ml Trypsin (Sigma, California, USA; T1426-500MG) and 1 unit/ml DNase I (Sigma, California, USA; AMPD1-1KT), then incubated in a shaking water bath at 32 °C for 10 min. Cells were collected by centrifugation at 500*g* for 2 min. The cell pellet was washed twice with DMEM and filtered through a 40 μm Nylon Cell Strainer (BD Falcon, NJ, USA; 352340) to separate cells from cell debris and other impurities. The cells were centrifuged at 1000 rpm for 5 min at 4 °C and cell pellets were re-suspended in 1ml PBS (Cytiva, MA, USA; SH30258.02). To remove red blood cells, 2 mL GEXSCOPETM Red Blood Cell Lysis Bufler (Singleron Biotechnologies, Nanjing, China) was added and incubated at 25 °C for 10 min. The mixture was then centrifuged at 1000 rpm for 5 min and cell pellet was re-suspended in PBS. Cell numbers were obtained by TC20 automated cell counter (Bio-Rad, California, USA).

Library preparation of scRNA-seq

scRNA-seq was performed on testes from WT, control and JQ1-treated mice by using the Singleron GEXSCOPE™ technique (Singleron Biotechnologies, Nanjing, China) following the protocol in Dura's description.[21] Each experimental group has only one sample. Briefly, the concentration of single-cell suspension was adjusted to 1×10^5 cells/mL in PBS (Cytiva, MA, USA; SH30258.02) and loaded onto a microfluidic chip (part of Singleron GEXSCOPETM Single Cell RNAseq Kit, Singleron Biotechnologies, Nanjing, China). scRNA-seq libraries were constructed according to manufacturer's instructions (Singleron Biotechnologies, Nanjing, China) and sequenced on Illumina HiSeq X Ten at Novogene (Beijing, China) with 150 bp paired end reads.

Data analysis of scRNA-Seq

Based on library preparation and sequencing of scRNA-seq above, each sample obtained two paired-end reads. Read 2 was separated by specific cell barcode information, and read 1 had alignment information based on Unique Molecular Identifier (UMI).[22] UMI-tools (v1.0.1) was used to align the fastq reads which contained UMIs ± cell barcodes, remove UMI sequences from fastq reads and appende UMIs to the read name. The processed data were mapped to the mouse reference genome (GRCm38.p6, Gencode) through STAR (v2.7.5a).[23] The gene expression data of each cell for all the samples were obtained by featureCounts software.[24]

The Seurat package (v3.1.0)[25] in R was used to screen cells according to the following three criteria: the number of genes detected in a single cell, the number of UMIs and the percentage of reads that map to the mitochondrial genome.[26] We filtered cells that have unique feature counts over 6000 or less than 1000 and mitochondrial counts >10%. The SCTransform function was performed to normalize and scale the data. The principal component analysis was performed on the scaled data to separate the cells. The PCs 1−30 were selected to perform the RunTSNE function[27] or RunUMAP function,[28] the FindNeighbors function and the FindClusters function (resolution = 0.8) to obtain the cell clusters. The FindAllMarkers function was used to identify unique cluster-specific marker genes. We chose the genes with the value of p_val_adj <0.05 and performed GO analysis using the clusterProfiler (v.3.16.0)[29] and org.Mm.eg.db (v3.11.1) package. Through the results about the cell-specific genes and the GO function enrichment analysis about cluster-specific marker genes, we determined the cell type of each cell cluster. Then we used jupyter notebook (v1.0) to show the results about the expression of cell-specific genes in different cell types.

Based on the highly variable genes obtained from Seurat, Monocle 3 was conducted to generate the pseudo-time trajectory for the different stages of germ cells.[30,31] We adopted the following three steps: choosing genes that define the progress of a cell, reducing data dimensionality and ordering cells along the trajectory to construct single-cell trajectories. The plot_cell_trajectory function was used to show the lines plots of pseudotime order with fitted curves of all the samples.

The function subset in Seurat package was used to obtain the cell numbers of each cell type. FindMarkers function in Seurat package was used to identify differentially expressed genes (DEGs) between different samples on the same cell types. DEGs were defined only if the adjusted *P* values and FDR were both <0.05, and a fold change (log2-transferred) was >1 or < −1 which presented as up-regulated and down-regulated genes respectively. According to the DEGs, we performed GO function enrichment analysis to find biological functions or pathways that are significantly related to the genes specifically expressed.

Purification of pacSC and RS from mouse testes

pacSC and RS from WT, control and JQ1-treated mouse testes were isolated using STA-PUT method based on Bellvé's description[32] with minor modifications. After obtaining the single-cell suspension, cells were collected by centrifugation at 500*g* for 2 min and re-suspended in 40 ml DMEM (Life Technologies, NY, USA; 11995-081) containing 0.5% BSA (Sangon Biotech, Shanghai, China; AD0023-100 g). Then the cells were separated by sedimentation velocity at unit gravity at 4 °C, using 2−4% BSA gradient in DMEM. Only fractions of the expected cell type and purity (≥75%) were pooled together. The purities of pacSC and RS were evaluated and identified by their morphological characterization and Q-PCR with germ cell type-specific marker genes (*Sycp3* for pacSC, and *Prm2 and Tnp1* for RS).

RNA extraction and Q-PCR

Total RNA was extracted using TRIzol (Invitrogen, NY, USA; 15596018) from mouse testicular tissues or isolated germ cells (pacSC and RS). Then reverse-transcribed into cDNA using a PrimeScript RT reagent kit (TaKaRa Bio, California, USA; RR036A). Q-PCR was performed on LightCycler®96 Instrument (Roche Diagnostics, Mannheim, Germany) using the SYBR Premix EX Taq kit (TaKaRa Bio, California, USA; RR820B), following the manufacturer's protocols. mRNA expression levels were normalized to mouse *Gapdh* mRNA

expression. Q-PCR primer sequences were listed in Table S2 (online).

Library preparation ATAC-seq

ATAC-seq was applied essentially following our previous description[20] and performed on pacSC and RS from WT, control and JQ1-treated mice, respectively. These six cell samples all had two replicates. The libraries were sequenced on Illumina HiSeq X Ten and NovaSeq 6000 at Novogene (Beijing, China) with 150 bp paired end reads.

Data analysis of ATAC-seq

After library preparation and sequencing of ATAC-seq, we got raw paired-end reads. Firstly, the software fastp (v.0.20.1)[33] was used for quality control and filtering the raw reads. Secondly, all reads for each sample were combined and aligned to mm10 (USCS version) with bowtie2 (v.2.4.1).[34] Thirdly, macs2 (v2.2.7.1)[35] was used to find peaks for each sample and deeptools (v3.4.3)[36] was applied to check the signal strength of the gene body (such as TSS and TES). Then Homer (v4.11)[37] was chosen to annotate the peaks and count peak distributions in promoter, exon, intron and intergenic regions. The differential peak regions were identified using DiffBind (v2.16.0) based on statistical mode DEseq2.[38] Homer (v4.11) was used to search and annotate the motifs in the differential peak regions. The transcript ID of the differential peak regions was converted to gene ID on David (v6.8). In addition, GO and KEGG analysis was also performed on David (v6.8). The list of meiotic DNA double strand break sites for the peaks was generated from previously published DMC1 ChIP-seq.[39]

Availability of data

The raw sequencing data (scRNA-seq and ATAC-seq) reported in this paper are available in the Genome Sequence Archive in the Beijing Institute of Genomics data center: CRA002896.

Statistical analysis

Statistical analysis was carried out using GraphPad Prism to assess differences between experimental groups. Statistical significance was analysed by Student's *t*-test and expressed as a *P*-value. *P*-values lower than 0.05 were considered to be statistically significant. *, $P < 0.05$; **, $P < 0.01$; ***, $P < 0.001$.

Results

Inhibition of BET bromodomain by JQ1 triggers male germ cell defects in mouse

To assess the possible effect of inhibition of super enhancer in spermatogenesis, 3 weeks juvenile C57BL/6 male mice were administered JQ1 (the mixture of (+)-JQ1, DMSO and 2-hydroxypropyl-b-cyclodextrin) (50 mg/kg once daily) or vehicle control (the mixture of DMSO and 2-hydroxypropyl-b-cyclodextrin) via *ip* injection daily for 3 weeks, and the records of mouse daily weight were shown in Figure. S1A. After the treatment, mice were sacrificed. Compared with control and WT mice (wild type mice of the same age without any treatment), JQ1-treated mice revealed a significant reduction in testicular volume (Fig. 1A). In terms of the testis weight, JQ1-treated mice showed a reduction to 68% of control and 67% of WT mice (Fig. 1B).

To examine the effect of JQ1 on various types of cells in the testis from a histological level, we performed hematoxylin and eosin staining, and the results demonstrated a reduction in the numbers of round spermatids and subsequent types of germ cells after JQ1 treatment, and some abnormal spermatids appeared to have large nuclei and abundant cytoplasm and symplasts, as indicated by black arrow (Fig. 1C), which was consistent with previous study.[19] These results suggest that the BET bromodomain inhibitor JQ1 could cause germ cell defects and affect testicular development in male mice.

Single-cell transcriptome profiling and cell type identification of JQ1-treated mouse testes

To investigate the cell-type-specific alterations in gene expression after JQ1 or control treatment at single-cell resolution, we performed single-cell RNA sequencing (scRNA-seq) on testes from WT, control and JQ1-treated mice by using the Singleron GEXSCOPE™ technique (Singleron Biotechnologies, Nanjing, China) following the protocol in Dura's description (Fig. S2A).[21] After obtaining high-throughput sequencing data of scRNA-seq, we first filtered the data, and screened out the cells with the number of feature RNA between 1000 and 6000 and the percentage of mitochondrial genes below 10% for further

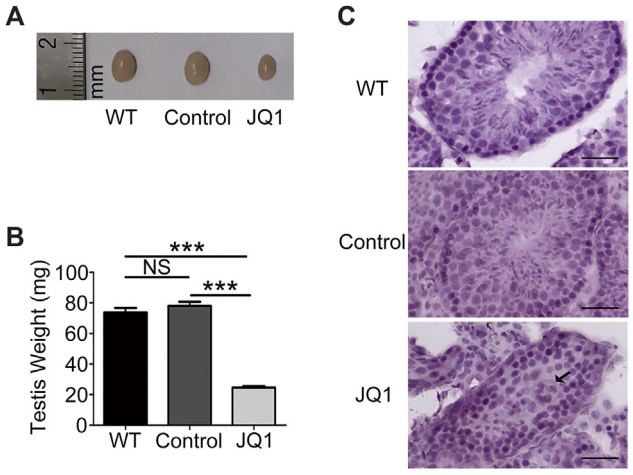

Figure 1 Inhibition of BET bromodomain reduces testis size and triggers germ cell defects. Testis morphology (**A**) and weight (**B**) of WT, control and JQ1-treated (50 mg/kg once daily) mice from 3 to 6 weeks. Data are presented as mean ± SEM. ***, $P < 0.001$; NS, $P > 0.05$. (**C**) Hematoxylin and eosin staining of testis seminiferous tubules from WT, control and JQ1-treated (50 mg/kg once daily) mice from 3 to 6 weeks. The abnormal spermatid with large nuclei and abundant cytoplasm and symplasts is shown by black arrow.

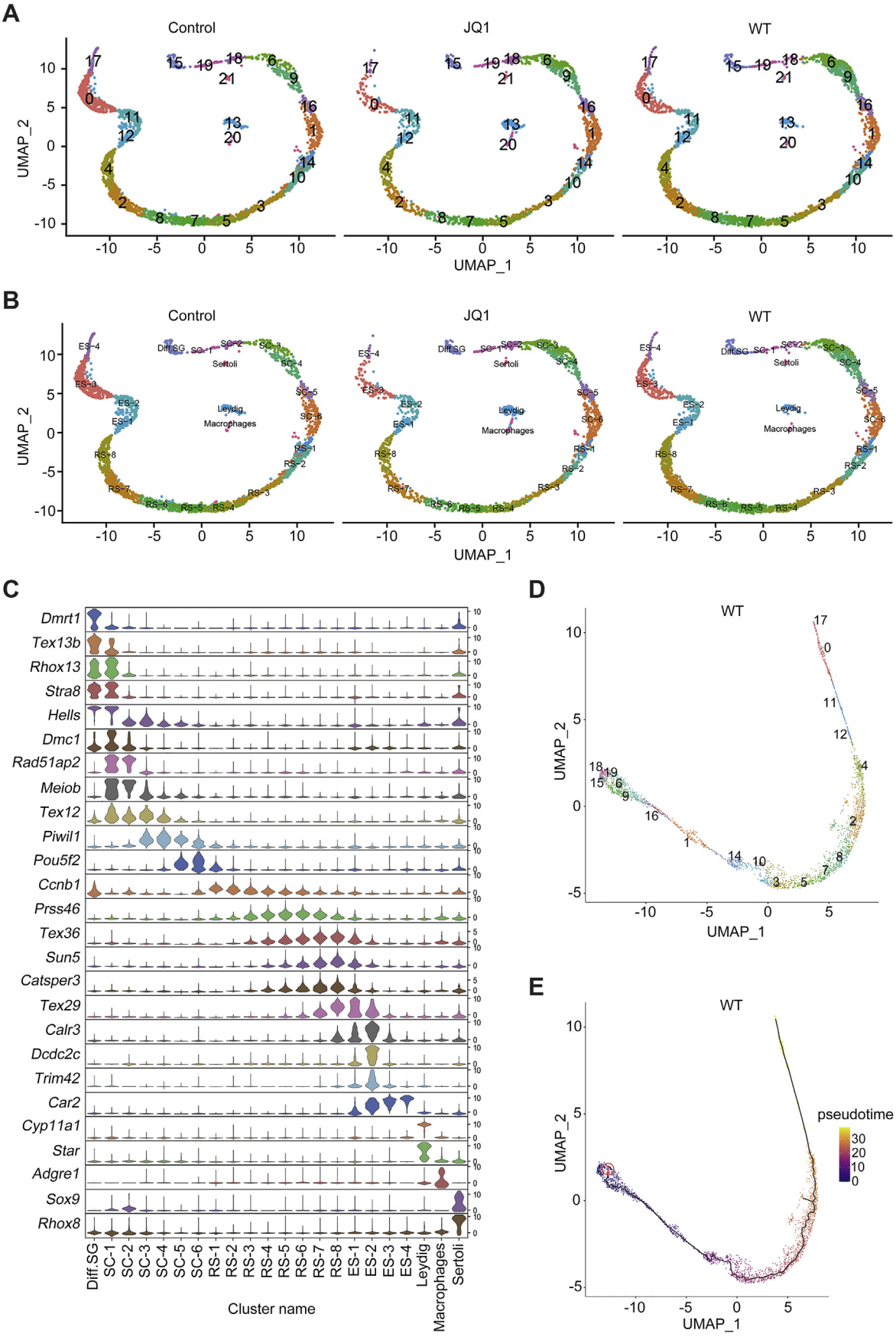
A
Control
JQ1
WT
UMAP_2
UMAP_1
B
Control
JQ1
WT
Diff.SG
Sertoli
Leydig
Macrophages
UMAP_2
UMAP_1
C
Dmrt1
Tex13b
Rhox13
Stra8
Hells
Dmc1
Rad51ap2
Meiob
Tex12
Piwil1
Pou5f2
Ccnb1
Prss46
Tex36
Sun5
Catsper3
Tex29
Calr3
Dcdc2c
Trim42
Car2
Cyp11a1
Star
Adgre1
Sox9
Rhox8
Diff.SG
SC-1
SC-2
SC-3
SC-4
SC-5
SC-6
RS-1
RS-2
RS-3
RS-4
RS-5
RS-6
RS-7
RS-8
ES-1
ES-2
ES-3
ES-4
Leydig
Macrophages
Sertoli
Cluster name
D
WT
UMAP_2
UMAP_1
E
WT
pseudotime
30
20
10
0
UMAP_2
UMAP_1

analysis (Fig. S2B). In total, we obtained 2 776, 2936 and 2291 cells from WT, control and JQ1-treated mouse testes, respectively.

To identify cell types, the non-linear dimensional reduction technique, t-distributed stochastic neighbor embedding (t-SNE) analysis[27] was applied. The results revealed that the testicular cells were all organized as 19 consecutive clusters and 3 separate clusters in three experimental samples (Fig. S2C). In addition, another dimension reduction technique, uniform manifold approximation and projection (UMAP),[28] was also performed in this study. UMAP demonstrated similar but slightly different results from t-SNE analysis (Fig. 2A).

Using previously determined cell type marker genes,[40–43] we annotated 19 clusters of germ cells which revealed the order of the cells corresponds to the developmental trajectory of spermatogenesis and 3 clusters composed of somatic cells (Fig. 2B). Specifically, cluster 15 representing differentiating spermatogonia (Diff. SG) (*Dmrt1*$^+$, *Tex13b*$^+$, *Rhox13*$^+$ and *Stra8*$^+$). Cluster 19, 18, 6, 9, 16 and 1 were identified as six different stages of spermatocytes (SC-1, SC-2, SC-3, SC-4, SC-5 and SC-6, respectively). Among them, SC-1 were preleptotene spermatocytes (*Rhox13*$^+$, *Stra8*$^+$ and *Dmc1*$^+$); SC-2 were a mixture of leptotene spermatocytes and zygotene spermatocytes (*Rad51ap2*$^+$ and *Meiob*$^+$); SC-3 and SC-4 were two successive stages of pachytene spermatocytes (pacSC) (*Piwil1*$^+$); SC-5 were diplotene spermatocytes (dipSC) (*Piwil1*$^+$ and *Pou5f2*$^+$); SC-6 were a mixture of diakinesis, metaphase, anaphase, telophase, and secondary spermatocytes (*Pou5f2*$^+$). Cluster 14, 10, 3, 5, 7, 8, 2 and 4 were corresponded to eight sequential stages of round spermatids (RS-1, RS-2, RS-3, RS-4, RS-5, RS-6, RS-7 and RS-8, respectively) (*Ccnb1*$^+$, *Prss46*$^+$, *Tex36*$^+$, *Sun5*$^+$ and *Catsper3*$^+$). Cluster 12, 11, 0 and 17 were four consecutive stages of elongating spermatids (ES-1, ES-2, ES-3 and ES-4, respectively) (*Calr3*$^+$, *Dcdc2c*$^+$, *Trim42*$^+$ and *Car2*$^+$). Cluster 13 were Leydig cells (*Cyp11a1*$^+$ and *Star*$^+$). Cluster 20 were macrophages (*Adgre1*$^+$). Cluster 21 were Sertoli cells (*Sox9*$^+$ and *Rhox8*$^+$) (Fig. 2C).

To confirm that the different stages of germ cells along a differentiation path, an orthogonal pseudotime analysis was conducted by using Monocle 3.[30,31] The data from WT (Fig. 2D, E), control (Fig. S2D) and JQ1-treated mice (Fig. S2E) were analyzed separately, and the results further supported our previous judgment on the classification of cell populations.

Unique gene-expression signatures of control and JQ1-treated mouse testes

Graph-based dimensionality reduction (Fig. 2A,B) showed that although the three samples consisted of the same cell types, the cell number and density of a certain cluster varied greatly. To quantify this difference, the cells in each cluster were counted and cell densities were calculated (Table S1 online). Compared with control mice, the cell densities of somatic cells and spermatocytes of JQ1-treated mice demonstrated a significant increase, especially in Leydig cells, macrophages, SC-3, SC-5 and SC-6. On the contrary, the cell densities of spermatid cells of JQ1-treated mice revealed a remarkable decrease, especially in ES-3 and ES-4 (Fig. 3A). These results indicate that the BET bromodomain inhibitor JQ1 can increase the numbers of somatic cells and spermatocytes and decrease the numbers of spermatid cells.

To better understand the influence of JQ1 on testicular cell development, we sought to explore the gene-expression changes involved in each cell types in the testis after JQ1 administration. First, DEGs among three experimental samples (WT, control and JQ1-treated) were identified and counted. Compared with control mice, DEGs down-regulated in JQ1-treated mice were principally involved in SC-6, RS-3, RS-4, RS-5, RS-6, RS-7 and Leydig clusters (Fig. 3B). To explore the impact of JQ1 on specific functional pathways in spermatogenesis, we performed GO analysis on the DEGs down-regulated in the above cell clusters of JQ1-treated mice. "spermatid development", "spermatid differentiation", "flagellated sperm motility", "sperm motility" were the four most frequently occurring biological processes, which were closely related to spermiogenesis and sperm maturation (Fig. 3C).

Compared with WT mice, DEGs were mainly contained in Diff. SG, SC-3, SC-6, RS-4, RS-5, RS-6 and ES-3 in JQ1-treated mice (Fig. S3A), which was slightly different from the results compared with control mice. Compared with WT mice, DEGs primarily appeared in SC-6 and ES-1 in control mice (Fig. S3B), which was an unexpected result. Control mice were injected intraperitoneally with a mixture of DMSO and 2-hydroxypropyl-b-cyclodextrin, which is widely employed as the vehicle control for both *in vitro*[44] and *in vivo*[19] studies. But there is not much research on its toxic and side effects. Our study surprisingly found that *ip* injection of the vehicle control could affect gene expression during meiosis and spermiogenesis in mice. Furthermore, functional enrichment analysis of DEGs illuminated that the vehicle control mainly affected some biological processes, such as "mRNA processing", "ribonucleoprotein complex biogenesis" and "RNA splicing" in SC-6 (Fig. S3C) and "mitochondrion organization" in ES-1 (Fig. S3D). In addition, "spermatid differentiation" and "spermatid development" biological processes were regulated in both SC-6 and ES-1 (Fig. S3C, D). These results indicate that the vehicle control has a certain solvent toxicity which will regulate the functions of germ cells. Therefore, in addition to the vehicle control group, it is necessary to add an untreated control group to detect the solvent toxicity.

Figure 2 Global patterns of single-cell transcriptome profiling and cell type identification. **(A)** UMAP plots showing 22 clusters of testicular cells. Left: Control mouse; Middle: JQ1 mouse; Right: WT mouse. **(B)** UMAP plots showing 19 clusters of germ cells and 3 clusters of somatic cells. Left: Control mouse; Middle: JQ1-treated mouse; Right: WT mouse. **(C)** Violin plots showing the expression levels of cell type marker genes based on RNA-seq analysis throughout 19 clusters of germ cells and 3 clusters of somatic cells. **(D–E)** Developmental pseudotime of male germ cells of WT mouse.

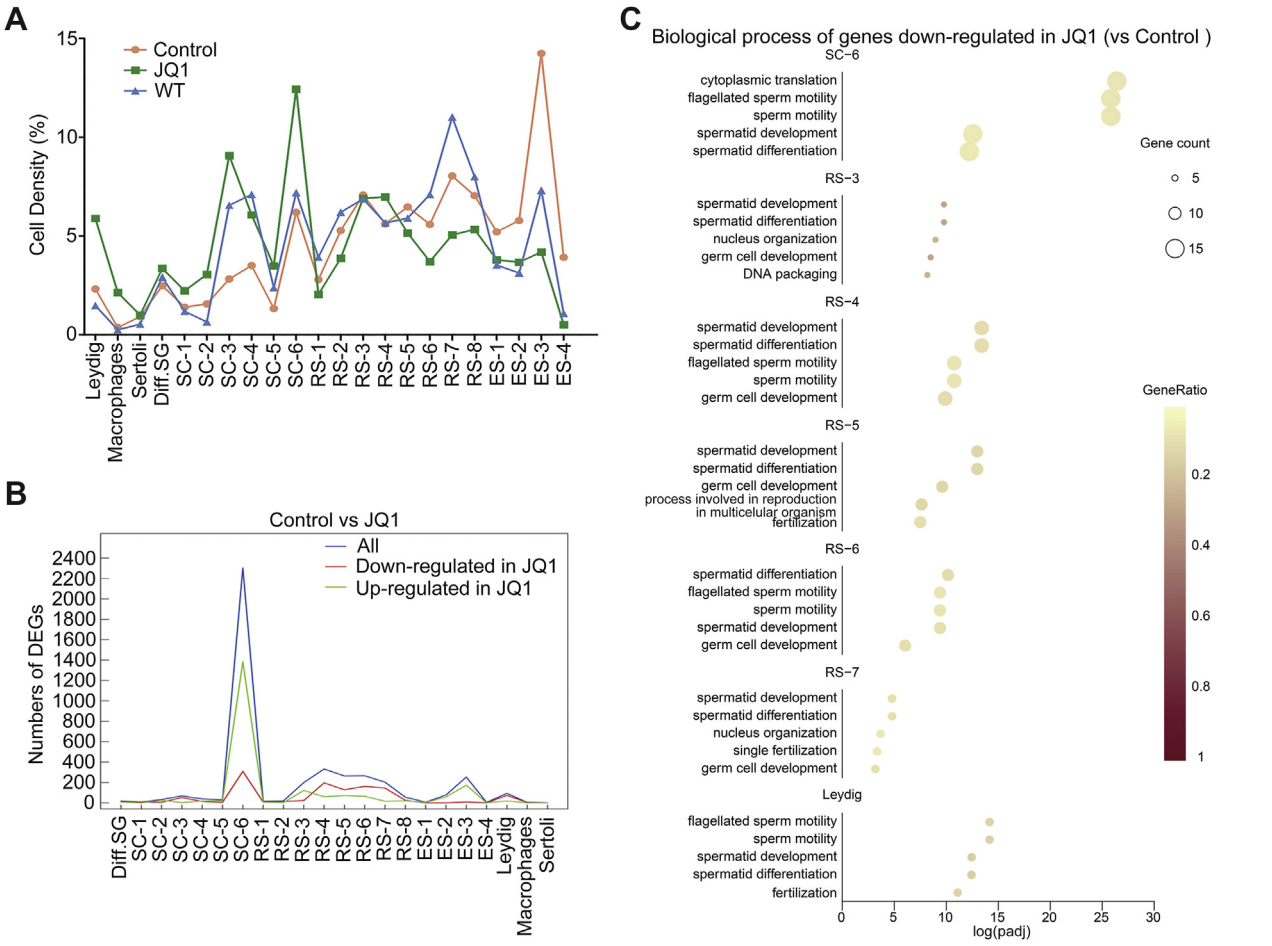

Figure 3 Unique gene-expression signatures of Control, JQ1-treated and WT mouse testes. **(A)** The cell density of each cell cluster from control, JQ1-treated and WT mice. **(B)** The numbers of DEGs between control and JQ1-treated mice. **(C)** First five GO terms of DEGs down-regulated in JQ1-treated group compared to control in seven cell clusters (inducing SC-6, RS-3, RS-4, RS-5, RS-6, RS-7 and Leydig).

Changes in DNA conformation in JQ1-treated mouse testes

To further understand the enfluence of JQ1 on specific functional pathways in spermatogenesis, we performed GO analysis on the DEGs in the remaining cell clusters between control and JQ1-treated mice. Notably, for genes down-regulated in JQ1-treated mice, ''nucleus organization'', ''DNA packaging'' and ''DNA conformation change'' were the three most frequently occurring biological processes, which occurred not only in germ cells (Diff. SG, SC-1, SC-2, SC-3, SC-4, SC-5, RS-1 and RS-2), but also in somatic cells (Macrophages) (Fig. 4A).

To verify the regulatory function of JQ1 on DNA conformation, we tested the RNA expression levels of some genes correlated with DNA conformation change in testicular cells. The results of real-time fluorescence-based quantitative PCR (Q-PCR) illuminated that the transcription levels of *Prm1*, *Prm2*, *Prm3*, *Tnp1*, *Tnp2* and *Hils1* genes were significantly reduced after JQ1 treatment (Fig. 4B). To explore whether this phenomenon also exists in specific germ cell types, such as pacSC and RS, we isolated and purified pacSC and RS from WT, control and JQ1-treated mice by using STA-PUT velocity sedimentation method[20,32,45] and validated the cell types and purities of these cells by morphological characterization (Fig. S4A) and Q-PCR with cell-type-specific markers (*Sycp3* for pacSC, and *Prm2* and *Tnp1* for RS) (Fig. S4B—D). Results revealed that the differential expressions of genes related to DNA conformation change in isolated cells were more remarkable, especially in RS (Fig. 4C, D). These phenomenons suggest that JQ1 treatment may affect the gene expression by changing the chromatin conformation, which in turn causes germ cell defects.

Changes in chromatin accessibility in JQ1-treated mouse testes

The open state of chromatin is one kind of chromatin conformation. To further investigate the effect of JQ1 on the change of chromatin conformation, we conducted assay for transposase accessible chromatin with high-throughput sequencing (ATAC-seq)[46] to measure chromatin accessibility in pacSC and RS in three groups, respectively. First, we found that the distributions of peaks on gene functional elements were different among six different cell samples and the

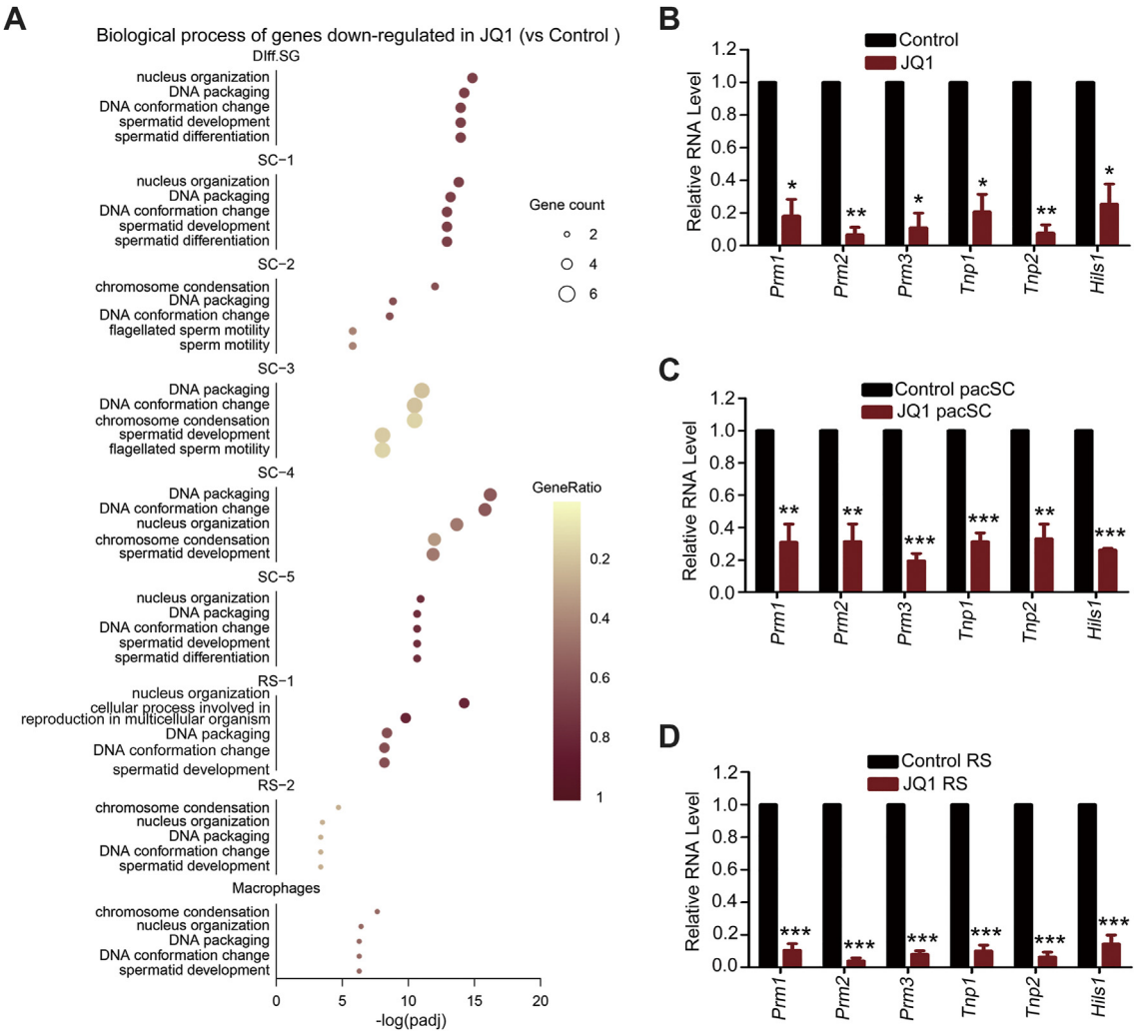

Figure 4 Changes in DNA conformation after JQ1 treatment. **(A)** First five GO terms of DEGs down-regulated in JQ1-treated group compared to control in nine cell clusters (inducing Diff. SG, SC-1, SC-2, SC-3, SC-4, SC-5, RS-1, RS-2 and Macrophages). **(B)** The relative expressions of *Prm1, Prm2, Prm3, Tnp1, Tnp2* and *Hils1* between control and JQ1-treated mouse testes were examined by Q-PCR. **(C)** The relative expressions of *Prm1, Prm2, Prm3, Tnp1, Tnp2* and *Hils1* between control pacSC and JQ1 pacSC were examined by Q-PCR. **(D)** The relative expressions of *Prm1, Prm2, Prm3, Tnp1, Tnp2* and *Hils1* between control RS and JQ1 RS were examined by Q-PCR. All data in (B—D) were presented as the means ± SEMs from at least three independent experiments. *, $P < 0.05$; **, $P < 0.01$; ***, $P < 0.001$.

proportion of the peaks involved in promoter in pacSC was higher than that in RS in the same experimental group (Fig. S5A). Then we found that the intensity of the accessible chromatin signal around transcriptional start sited (TSS) and transcriptional elongation site (TES) decreased as germ cell development, and the intensity in control group was stronger than that in JQ1-treated group, while that in WT group was the weakest (Fig. 5A). TF motif analysis revealed that differentially accessible chromatin regions between control pacSC and JQ1 pacSC and between control RS and JQ1 RS were enriched with same TF motifs, like NFY, KLF1, Sp2, Sp1 and Sp5, although *P*-values were slightly different (Fig. 5B). Meiotic recombination is initiated by the introduction of DNA double-stranded breaks (DSBs). Thus, we compared the numbers of accessible meiotic DSB sites among six samples, and unexpectedly found that the number of accessible meiotic DSB sites of JQ1 pacSC was lower than that of control pacSC, while the number of accessible meiotic DSB sites of JQ1 RS was slightly higher than that of control RS (Fig. 5C). These results suggested that JQ1 treatment may affect spermatogenesis by regulating meiotic recombination. GO analysis on the differentially accessible chromatin regions between control pacSC and JQ1 pacSC showed that differentially peaks took part in multiple functional pathways related to chromatin conformation, including "DNA repair", "covalent chromatin modification", "organelle fission", "histone modification" and so on (Fig. 5D). KEGG analysis showed that the differentially accessible chromatin regions between control pacSC and JQ1 pacSC were mainly involved in "Protein processing in endoplasmic reticulum", "Huntington disease" and "Parkinson disease" (Fig. 5E). In addition, GO analysis on the differentially accessible chromatin regions between WT pacSC and control pacSC showed that the vehicle control may affects the chromatin

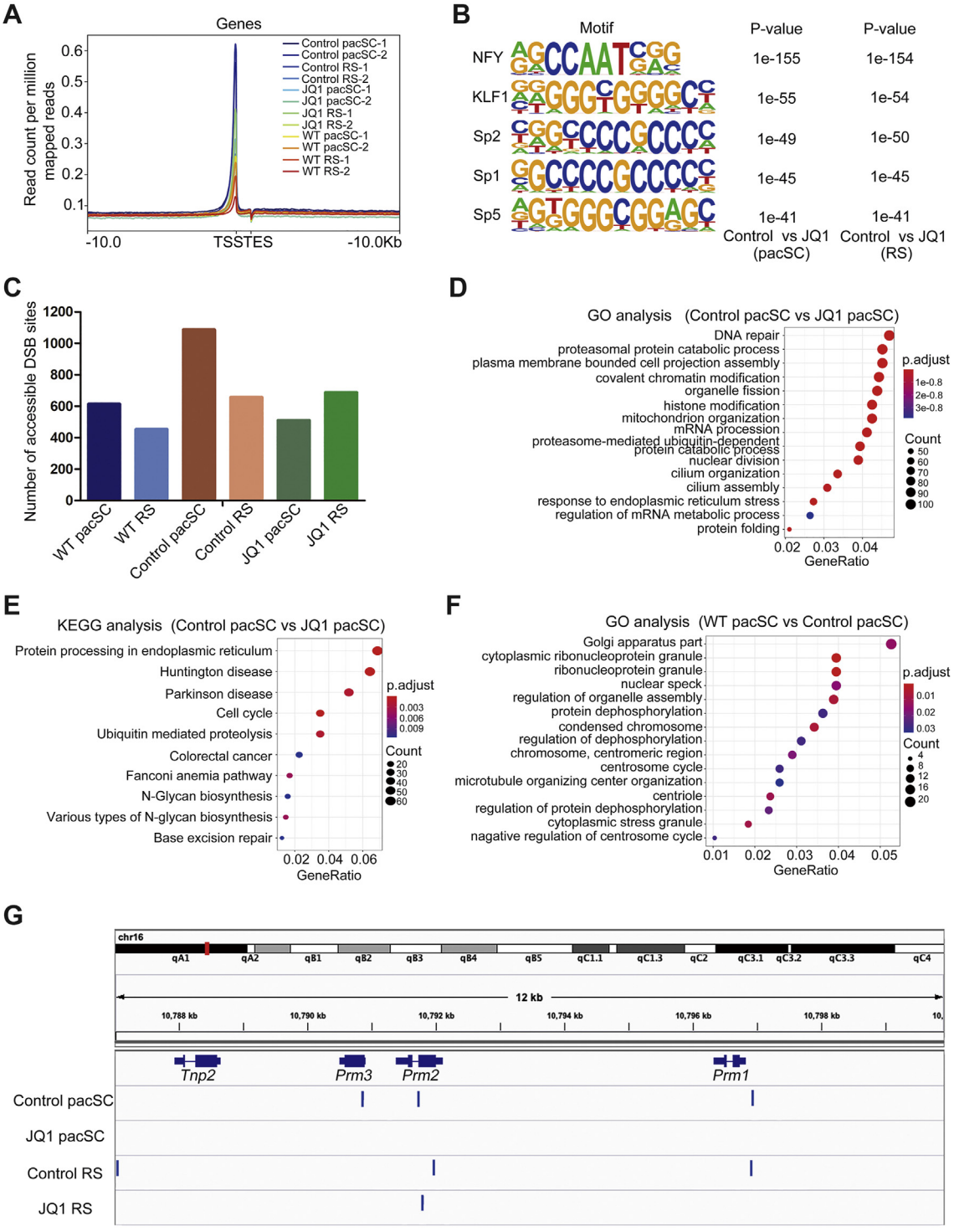

Figure 5 Changes in chromatin accessibility after JQ1 treatment. **(A)** The intensity of the accessible chromatin signal around TSS and TES of pacSC and RS from control, JQ1-treated and WT mice. **(B)** TF motif analysis on differentially accessible chromatin regions between control pacSC and JQ1 pacSC and between control RS and JQ1 RS. **(C)** The numbers of accessible meiotic DSB sites among six samples. **(D)** GO analysis on the differentially accessible chromatin regions between control pacSC and JQ1 pacSC. **(E)** KEGG pathway analysis on the differentially accessible chromatin regions between control pacSC and JQ1 pacSC. **(F)** GO analysis on the differentially accessible chromatin regions between WT pacSC and control pacSC. **(G)** The accessibility of *Prm1, Prm2, Prm3* and *Tnp2* genes which were located on chromosome 16.

accessibility of genes related to organelle function (Fig. 5F). Since chromatin accessibility is always correlated with gene expression, and we have confirmed that JQ1 could affect the RNA expression levels of six genes (*Prm1, Prm2, Prm3, Tnp1, Tnp2* and *Hils1*) correlated with DNA conformation change by scRNA-seq data analysis and Q-PCR technology. We explored the accessibility of four genes (*Prm1, Prm2, Prm3* and *Tnp2*) related to DNA conformation change on chromosome 16 and found that the accessibility of these genes decreased after JQ1 treatment (Fig. 5G). These results demonstrated that JQ1 treatment may regulate gene expression by reducing the chromatin accessibility of pacSC and RS.

Discussion

Effective contraception is needed for reproductive health.[47] To achieve the goal of birth control, various methods of regulating fertility must be available. In many societies, men are ready to share the responsibility of contraception more equally with their partners.[48] Therefore, the development of new and effective methods of male contraceptive methods has become a priority.

Previous studies have shown that BET bromodomain inhibitor JQ1 could penetrate the blood-testis barrier, and JQ1 treatment would result in germ cell defects and a reduction of sperm motility.[19] Here, we further investigated the effect of JQ1 on gene transcription in each type of germ cell and somatic cell from the single-cell resolution. In our work, the cell type of each cell population and differentiation path of germ cells showed no difference among WT, control and JQ1-treated group (Fig. 2, S1). So we focused our attention on the changes of each cell population and found that treatment of JQ1 would lead to remarkable increases of cell densities in somatic cells (Leydig cells and macrophages) and spermatocytes (SC-3, SC-5 and SC-6) and significant reductions of cell densities in spermatid cells (ES-3 and ES-4) (Fig. 3A). These results indicate that the BET bromodomain inhibitor JQ1 can not only regulate spermatogenesis, but also change the testicular microenvironment by regulating somatic cells. Previous studies have shown that spermatogonial differentiation requires testicular macrophages express spermatogonial proliferation- and differentiation-inducing factors, and fewer spermatogonia are contained in macrophages-depleted testes.[49] Then what happens if there is an increase of macrophages in the testis, will it promote the spermatogonia differentiation, resulting in more spermatocytes? Under the condition of JQ1 treatment, whether this mechanism also exists, which needs further study.

Previous biophysical experiments have revealed that BET-family bromodomains have acetyl-lysine binding site, which promotes BET-family protein bind to nucleosomes.[50] Furthermore, BRDT regulates the global chromatin organization of spermatocyte chromosomes and the local histone modifications of the chromatin approximate to the synaptonemal complex.[4] However, BET bromodomain inhibitor JQ1 could selectively bind to the acetyl-lysine binding site of BET-family bromodomains and displace BET-family protein from nuclear chromatin.[18] To verify whether JQ1 regulates spermatogenesis by modulating chromatin oaganization, we performed GO functional enrichment analysis on the DEGs of each cell population between control and JQ1-treated group. We found that the DEGs down-regulated in JQ1-treated mouse were enriched in "spermatid development" and "spermatid differentiation" biological processes in the majority of cell clusters (Fig. 3C, 4A). While at early developmental stages (Diff. SG, SC-1, SC-2, SC-3, SC-4, SC-5, RS-1 and RS-2), DEGs down-regulated in JQ1-treated mouse were also enriched in ''DNA conformation change'' biological process (Fig. 4A). These results indicate that JQ1 may regulate the expressions of genes associated with spermatid development by affecting the chromatin conformation of germ cells in the early developmental stage.

The open state of chromatin is also a form of chromatin conformation and is closely related to gene transcription. With the advent of ATAC-seq technology, researchers can easily obtain the chromatin accessibility of experimental samples.[46] Since full synapses of homologous chromosomes appear in pacSC, and spermiogenesis (the final stage of spermatogenesis) begins from RS. We purified pacSC and RS from WT, control and JQ1-treated group and performed ATAC-seq on these cell samples, respectively. ATAC-seq data further demonstrated that treatment of JQ1 could result in changes of chromatin accessibility (Fig. 5). In general, our results revealed that JQ1 regulated gene expression by changing chromatin conformation in mouse spermatogenesis, which ultimately led to germ cell defects and a remarkable reduction of sperm motility.

In addition, the mixture of DMSO and 2-hydroxypropyl-b-cyclodextrin was extensively used as a vehicle control in biological and medical experiments. But in this study, we found that the mixture had a certain solvent toxicity. The mixture could result in a large number of DEGs appear in SC-6 and ES-1 (Fig. S3B) and affect the chromatin accessibility of genes related to organelle function (Fig. 5F). Therefore, when the mixture is used as vehicle control group, it is necessary to pay attention to the dosage and add an untreated control group to detect the solvent toxicity.

Author contributions

X.W. and S.G. performed experiments with assistance from C.Z., X.Z, G.W., Z.L and Y.H.; M.S. performed data analysis with assistance from X.W., S.C. and G.X.; F.S and E.D. designed the project; X.W., M.S., F.S and E.D. wrote and reviewed the manuscript.

Conflict of interests

The authors declare that they have no conflict of interests.

Funding

This study was supported by the National Key Research and Development Program of China (No. 2018YFC1003500); and the National Natural Science Foundation of China (No. 81901528).

Abbreviations

ATAC-seq	the assay for transposase accessible chromatin with high-throughput sequencing
BET	the bromodomain and extra-terminal domain
Control/vehicle control	the mixture of DMSO and 2-hydroxypropyl-b-cyclodextrin
DEGs	differentially expressed genes
Diff. SG	differentiating spermatogonia
dipSC	diplotene spermatocytes
DSB	DNA double-stranded break
ES	elongating spermatids
GO	Gene Ontology
ip	intraperitoneal
JQ1	the mixture of (+)-JQ1, DMSO and 2-hydroxypropyl-b-cyclodextrin
pacSC	pachytene spermatocytes
Q-PCR	real-time fluorescence-based quantitative PCR
RS	round spermatids
SC	spermatocytes
scRNA-seq	Single-cell RNA sequencing
TES	transcriptional elongation site
TF	transcription factor
t-SNE	t-distributed stochastic neighbor embedding
TSS	transcriptional start site
UMAP	uniform manifold approximation and projection
UMI	Unique Molecular Identifier
WT	wild type

Appendix A. Supplementary data

Supplementary data to this article can be found online at https://doi.org/10.1016/j.gendis.2020.12.012.

References

1. Nishimura H, L'Hernault SW. Spermatogenesis. *Curr Biol*. 2017;27(18):R988—R994.
2. Clermont Y. Kinetics of spermatogenesis in mammals: seminiferous epithelium cycle and spermatogonial renewal. *Physiol Rev*. 1972;52(1):198—236.
3. White-Cooper H, Davidson I. Unique aspects of transcription regulation in male germ cells. *Cold Spring Harb Perspect Biol*. 2011;3(7):a002626.
4. Manterola M, Brown TM, Oh MY, Garyn C, Gonzalez BJ, Wolgemuth DJ. BRDT is an essential epigenetic regulator for proper chromatin organization, silencing of sex chromosomes and crossover formation in male meiosis. *PLoS Genet*. 2018;14(3):e1007209.
5. Gaucher J, Boussouar F, Montellier E, et al. Bromodomain-dependent stage-specific male genome programming by Brdt. *EMBO J*. 2012;31(19):3809—3820.
6. Shang E, Nickerson HD, Wen D, Wang X, Wolgemuth DJ. The first bromodomain of Brdt, a testis-specific member of the BET sub-family of double-bromodomain-containing proteins, is essential for male germ cell differentiation. *Development*. 2007;134(19):3507—3515.
7. Voigt P, Reinberg D. BRD4 jump-starts transcription after mitotic silencing. *Genome Biol*. 2011;12(11):133.
8. Shang E, Salazar G, Crowley TE, et al. Identification of unique, differentiation stage-specific patterns of expression of the bromodomain-containing genes Brd2, Brd3, Brd4, and Brdt in the mouse testis. *Gene Expr Patterns* . 2004;4(5):513—519.
9. Bryant JM, Donahue G, Wang X, et al. Characterization of BRD4 during mammalian postmeiotic sperm development. *Mol Cell Biol*. 2015;35(8):1433—1448.
10. Dawson MA, Prinjha RK, Dittmann A, et al. Inhibition of BET recruitment to chromatin as an effective treatment for MLL-fusion leukaemia. *Nature*. 2011;478(7370):529—533.
11. Lovén J, Hoke HA, Lin CY, et al. Selective inhibition of tumor oncogenes by disruption of super-enhancers. *Cell*. 2013;153(2):320—334.
12. Whyte WA, Orlando DA, Hnisz D, et al. Master transcription factors and mediator establish super-enhancers at key cell identity genes. *Cell*. 2013;153(2):307—319.
13. Hnisz D, Abraham BJ, Lee TI, et al. Super-enhancers in the control of cell identity and disease. *Cell*. 2013;155(4):934—947.
14. Vahedi G, Kanno Y, Furumoto Y, et al. Super-enhancers delineate disease-associated regulatory nodes in T cells. *Nature*. 2015;520(7548):558—562.
15. Parker SC, Stitzel ML, Taylor DL, et al. Chromatin stretch enhancer states drive cell-specific gene regulation and harbor human disease risk variants. *Proc Natl Acad Sci U S A*. 2013;110(44):17921—17926.
16. Achour M, Le Gras S, Keime C, et al. Neuronal identity genes regulated by super-enhancers are preferentially down-regulated in the striatum of Huntington's disease mice. *Hum Mol Genet*. 2015;24(12):3481—3496.
17. Shi J, Vakoc CR. The mechanisms behind the therapeutic activity of BET bromodomain inhibition. *Mol Cell*. 2014;54(5):728—736.
18. Filippakopoulos P, Qi J, Picaud S, et al. Selective inhibition of BET bromodomains. *Nature*. 2010;468(7327):1067—1073.
19. Matzuk MM, McKeown MR, Filippakopoulos P, et al. Small-molecule inhibition of BRDT for male contraception. *Cell*. 2012;150(4):673—684.
20. Luo Z, Wang X, Jiang H, et al. Reorganized 3D genome structures support transcriptional regulation in mouse spermatogenesis. *iScience*. 2020;23(4):101034.
21. Dura B, Choi JY, Zhang K, et al. scFTD-seq: freeze-thaw lysis based, portable approach toward highly distributed single-cell 3' mRNA profiling. *Nucleic Acids Res*. 2019;47(3):e16.
22. Smith T, Heger A, Sudbery I. UMI-tools: modeling sequencing errors in Unique Molecular Identifiers to improve quantification accuracy. *Genome Res*. 2017;27(3):491—499.
23. Dobin A, Davis CA, Schlesinger F, et al. STAR: ultrafast universal RNA-seq aligner. *Bioinformatics*. 2013;29(1):15—21.
24. Liao Y, Smyth GK, Shi W. featureCounts: an efficient general purpose program for assigning sequence reads to genomic features. *Bioinformatics*. 2014;30(7):923—930.
25. Gribov A, Sill M, Lück S, et al. SEURAT: visual analytics for the integrated analysis of microarray data. *BMC Med Genomics*. 2010;3:21.
26. Butler A, Hoffman P, Smibert P, Papalexi E, Satija R. Integrating single-cell transcriptomic data across different conditions, technologies, and species. *Nat Biotechnol*. 2018;36(5):411—420.
27. van der Maaten L, Hinton G. Visualizing Data using t-SNE. *J Mach Learn Res*. 2008;9:2579—2605.
28. McInnes L, Healy J, Melville J. UMAP: uniform manifold approximation and projection for dimension reduction. *J Open Source Software*. 2018;3(29):861.
29. Yu G, Wang LG, Han Y, He QY. clusterProfiler: an R package for comparing biological themes among gene clusters. *OMICS*. 2012;16(5):284—287.
30. Qiu X, Mao Q, Tang Y, et al. Reversed graph embedding resolves complex single-cell trajectories. *Nat Method*. 2017;14(10):979—982.
31. Cao J, Spielmann M, Qiu X, et al. The single-cell transcriptional landscape of mammalian organogenesis. *Nature*. 2019;566(7745):496—502.

32. Bellvé AR, Cavicchia JC, Millette CF, O'Brien DA, Bhatnagar YM, Dym M. Spermatogenic cells of the prepuberal mouse. Isolation and morphological characterization. *J Cell Biol*. 1977;74(1):68—85.
33. Chen S, Zhou Y, Chen Y, Gu J. fastp: an ultra-fast all-in-one FASTQ preprocessor. *Bioinformatics*. 2018;34(17):i884—i890.
34. Langmead B, Salzberg SL. Fast gapped-read alignment with Bowtie 2. *Nat Method*. 2012;9(4):357—359.
35. Zhang Y, Liu T, Meyer CA, et al. Model-based analysis of ChIP-seq (MACS). *Genome Biol*. 2008;9(9):R137.
36. Ramírez F, Ryan DP, Grüning B, et al. deepTools2: a next generation web server for deep-sequencing data analysis. *Nucleic Acids Res*. 2016;44(W1):W160—W165.
37. Heinz S, Benner C, Spann N, et al. Simple combinations of lineage-determining transcription factors prime cis-regulatory elements required for macrophage and B cell identities. *Mol Cell*. 2010;38(4):576—589.
38. Love MI, Huber W, Anders S. Moderated estimation of fold change and dispersion for RNA-seq data with DESeq2. *Genome Biol*. 2014;15(12):550.
39. Smagulova F, Gregoretti IV, Brick K, Khil P, Camerini-Otero RD, Petukhova GV. Genome-wide analysis reveals novel molecular features of mouse recombination hotspots. *Nature*. 2011;472(7343):375—378.
40. Hermann BP, Cheng K, Singh A, et al. The mammalian spermatogenesis single-cell transcriptome, from spermatogonial stem cells to spermatids. *Cell Rep*. 2018;25(6):1650—1667.
41. Lu Y, Oura S, Matsumura T, et al. CRISPR/Cas9-mediated genome editing reveals 30 testis-enriched genes dispensable for male fertility in mice. *Biol Reprod*. 2019;101(2):501—511.
42. Chen Y, Zheng Y, Gao Y, et al. Single-cell RNA-seq uncovers dynamic processes and critical regulators in mouse spermatogenesis. *Cell Res*. 2018;28(9):879—896.
43. Wen L, Tang F. Human germline cell development: from the perspective of single-cell sequencing. *Mol Cell*. 2019;76(2):320—328.
44. Sankpal UT, Abdelrahim M, Connelly SF, et al. Small molecule tolfenamic acid inhibits PC-3 cell proliferation and invasion in vitro, and tumor growth in orthotopic mouse model for prostate cancer. *Prostate*. 2012;72(15):1648—1658.
45. Gan H, Wen L, Liao S, et al. Dynamics of 5-hydroxymethylcytosine during mouse spermatogenesis. *Nat Commun*. 2013;4:1995.
46. Buenrostro JD, Wu B, Chang HY, Greenleaf WJ. ATAC-seq: a method for assaying chromatin accessibility genome-wide. *Curr Protoc Mol Biol*. 2015;109:21—29.
47. Anderson RA, Baird DT. Male contraception. *Endocr Rev*. 2002;23(6):735—762.
48. Martin CW, Anderson RA, Cheng L, et al. Potential impact of hormonal male contraception: cross-cultural implications for development of novel preparations. *Hum Reprod*. 2000;15(3):637—645.
49. DeFalco T, Potter SJ, Williams AV, Waller B, Kan MJ, Capel B. Macrophages contribute to the spermatogonial niche in the adult testis. *Cell Rep*. 2015;12(7):1107—1119.
50. Miller TC, Simon B, Rybin V, et al. A bromodomain-DNA interaction facilitates acetylation-dependent bivalent nucleosome recognition by the BET protein BRDT. *Nat Commun*. 2016;7:13855.